Supporting Information

Distribution of alkali cations near Cu (111) surface in aqueous solution

Cong Xi,[ab] Fan Zheng,[b] Guoping Gao,[b] Meng Ye,[b] Cunku Dong,[a] Xi-Wen Du*[a] and Lin-Wang Wang*[bc]

[a]Institute of New Energy Materials, School of Materials Science and Engineering, Tianjin University, Tianjin 30072, People's Republic of China

[b]Materials Science Division, Lawrence Berkeley National Laboratory, Berkeley, California, 94720, USA

[c]Joint Center for Artificial Photosynthesis and Materials Science Division, Lawrence Berkeley National Laboratory, Berkeley, California, 94720, USA.

1. Computational Details

The Vienna Ab initio Simulation Package (VASP)[1-2] was employed for all calculations. Electronic structure calculations were performed within the DFT framework and the projector augmented wave (PAW) potentials were used to account for the nuclei–electron interactions[3]. The generalized gradient approximation (GGA)[4] with the Perdew–Burke–Ernzerhof (PBE) functional[5] was used to represent the electron exchange–correlation interactions. Grimme's DFT-D3 correction method was used to describe the van der Waals (vdW) effects.[6] The kinetic energy cutoff for plane wave expansions was set 500 eV. The convergence criteria for energy and force during geometrical optimization were set to 10^{-5} eV and 0.03 eV A^{-1}, respectively. The vacuum space of 23 Å was applied to avoid the interactions along the z-direction. ab initio molecular dynamics (AIMD) simulations were performed to examine the position of the cation on neutral and charged Cu (111) electrode. We carried out at least 50 ps of AIMD for each structure at 300K with time step 1 fs and Nose Hoover thermostat was employed for all simulations. The MD simulations used only the gamma point of the Brillouin zone with no consideration of symmetry. Here, we simulate the electrolyte/Cu (111) interface with 36 explicit water molecules (7 layers, 1.8 nm high) on a 3$\sqrt{3}$×3 Cu (111) slab (3 layers, 6 nm^2 in area).

For free energy calculation, we integrated ensemble average force on Na in z direction falling from infinity to the surface of Cu (111), over configurations sampled from a molecular dynamics according

to thermodynamic integration method.[7-8] Consider system when Na is in infinity as state A, and the system when Na is close to the interface as state B, with potential energies U_A and U_B, respectively. A new potential energy function is defined as:

$$U(\lambda) = U_A + \lambda (U_B - U_A) \tag{1}$$

Here, λ is defined as a coupling parameter with a value between 0 and 1. the partition function of the system can be written as:

$$Q(N,V,T,\lambda) = \sum_s \exp [- U_s(\lambda)/kT] \tag{2}$$

In this notation, k is the Boltzmann constant and $U_s(\lambda)$ is the potential energy of state s in the ensemble with potential energy function $U(\lambda)$ as defined above. The free energy of this system is defined as:

$$G(N,V,T,\lambda) = - kT \ln Q(N,V,T,\lambda) \tag{3}$$

If we take the derivative of G with respect to λ, we will get that it equals the ensemble average of the derivative of potential energy with respect to λ.

$$\Delta G(A\rightarrow B) = \int_0^1 \frac{\partial G(\lambda)}{\partial \lambda} d\lambda = - \int_0^1 \frac{kT \partial Q}{Q \partial \lambda} d\lambda = \int_0^1 \frac{kT}{Q} \sum_s \exp\left[- \frac{U_s(\lambda)}{kT} \right] \frac{\partial U_s(\lambda)}{\partial \lambda} d\lambda = \int_0^1 \left\langle \frac{\partial U(\lambda)}{\partial \lambda} \right\rangle_\lambda d\lambda = \int_0^1 \langle F \rangle_\lambda d\lambda \tag{4}$$

The change in free energy of Na between states A and B can thus be computed from the integral of the ensemble averaged force in z direction over the coupling parameter λ.

2. Notes for chemical potential derivation of 2D and 3D systems.

The single particle density of states in 3D system is given by

$$\rho_{3D}(\epsilon) = \frac{V}{4\pi^2} \left(\frac{2m}{\hbar^2} \right)^{\frac{3}{2}} \epsilon^{\frac{1}{2}} \tag{5}$$

and the (canonical) partition function for a single particle is:

$$z = \sum_k e^{- \beta \epsilon_k} \tag{6}$$

Hence, z in the bulk system in Eq. (6) is given by

$$z_{3D} = \frac{V}{4\pi^2} \left(\frac{2m}{\hbar^2} \right)^{3/2} \int_0^\infty \epsilon^{1/2} e^{- \beta \epsilon} d\epsilon = \frac{V}{4\pi^2} \left(\frac{2mkT}{\hbar^2} \right)^{3/2} \int_0^\infty x^{1/2} e^{- x} dx = V \left(\frac{mkT}{2\pi\hbar^2} \right)^{3/2} \tag{7}$$

Where β is integral factor and equals $1/kT$. Therefore, the chemical potential of single particle in 3D system is:

$$\mu_{3D} = -kT \ln z_{3D} = -kT \ln \left[\frac{1}{n}\left(\frac{mkT}{2\pi\hbar^2}\right)^{3/2}\right] \tag{8}$$

Similarly, the density of states in 2D system is:

$$\rho_{2D}(\epsilon) = \frac{Am}{2\pi\hbar^2} \tag{9}$$

Thus, z for 2D system in Eq. (6) is given by

$$z_{2D} = \frac{Am}{2\pi\hbar^2}\int_0^{\infty} e^{-\beta\epsilon} d\epsilon = \frac{AmkT}{2\pi\hbar^2}\int_0^{\infty} e^{-\epsilon} d\epsilon \quad = \frac{AmkT}{2\pi\hbar^2} \tag{10}$$

So, the chemical potential of single particle in 2D system is:

$$\mu_{2D} = -kT \ln z_{2D} = -kT \ln \left(\frac{mkT}{\sigma \cdot 2\pi\hbar^2}\right) \tag{11}$$

3. Notes for error bar of the average force.

We use correlation-time analysis to estimate uncertainty in force averages of cation.[9] The auto-correlation function for dynamic simulation is defined as:

$$f(\tau) = \frac{\sum_0^{t-\tau}(F_{z,(t+\tau)} - F_{z,ave})(F_{z,t} - F_{z,ave})}{(t-\tau)\sigma^2} \tag{12}$$

where t is dynamic simulation time, F_z is the force of cation in z direction, $F_{z,ave}$ and σ^2 are average force and variance through time t, respectively. The $F_{z,ave}$ is estimated via:

$$F_{z,ave} = \frac{\sum_0^{t} F_{z,t}}{t} \tag{13}$$

and σ^2 is defined as the average squared deviation from the mean:

$$\sigma^2 = \frac{\sum_0^{t}(F_{z,t} - F_{z,ave})^2}{t} \tag{14}$$

The autocorrelation time τ_0 quantifies the amount of time necessary for simulated values of F_z to lose their "memory" of earlier values. Thus, we can roughly say that the correlation time is smallest τ value for which $f(\tau) \ll 1$ for all subsequent times (within noise). In this work, the correlation time was fit to an exponential to find the appropriate τ_0 and the error was obtained via:

$$\text{error} = \sigma\sqrt{\frac{\tau_0}{t}} \tag{15}$$

where σ is the standard deviation, i.e., the square root of the variance.

4. The Figures in the supporting information (Fig. S1 ~ Fig. S5)

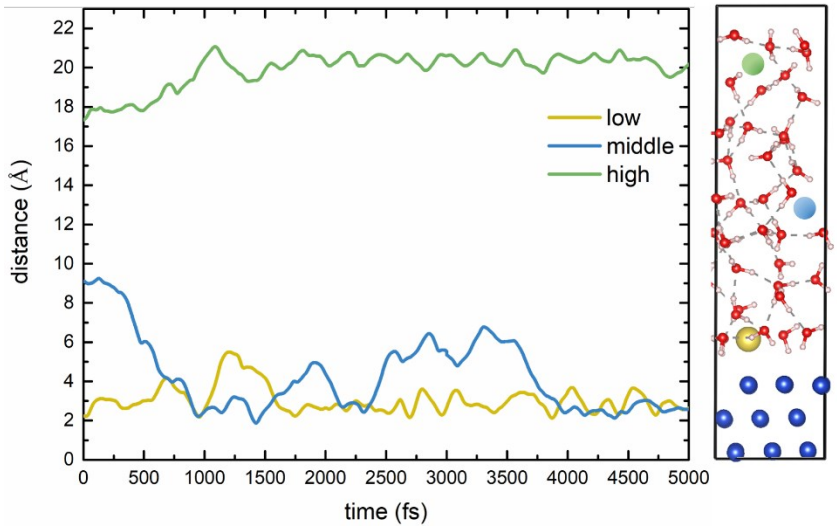

Figure S1. The change of distance between Na and the first layer of Cu with time in ab-initio MD. The yellow, blue and green curves in the left figure and balls in the right structure represent the initio Na is put 2.3 Å (low), 9.2 Å(middle), and 16.3 Å(high) from the bottom substrate, respectively. Na diffused ~3 Å away from the Cu regardless of the initio positions within 4 ps.

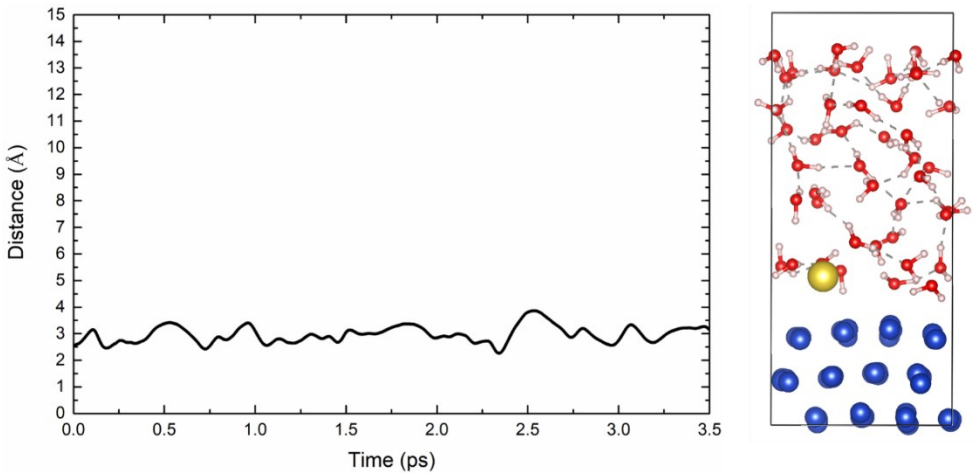

Figure S2. Na-first layer Cu distance versus time on a neutral 4x4 Cu (111) surface, with last structure image of MD simulation on the right.

In regard to the supercell size convergence, the balance between the computational feasibility and the size convergence must be considered very carefully. We believe our 3x3 supercell is sufficient. Many previous theoretical studies have been based on the 3x3 Cu supercell.[10-13] Nevertheless, to test the size effect, we have used ab initio molecular dynamics simulations to test Cu-Na distance on a neutral 4x4 Cu (111) surface, with about 15 Å space filled with 43 explicit water, as shown in the figure above. Na stays stably at about 3 Å above the first layer of Cu surface in 3.5 ps, which agrees with our 3x3 Cu supercell calculation (Fig.1 in the main text). We thus believe 3x3 Cu supercell should be good enough for our purpose, and there are no strong image-image interactions and correlation effects.

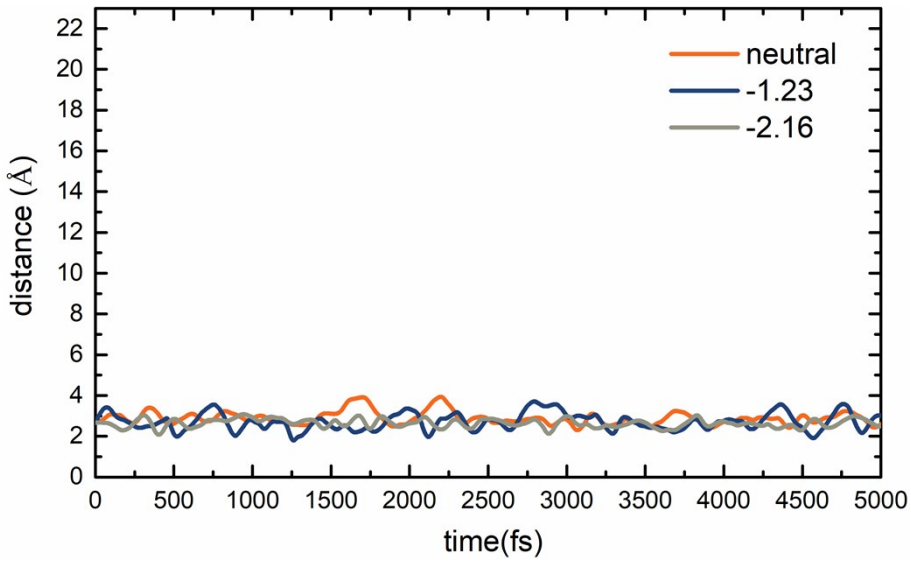

Figure S3. The change of distance over time between Na and the first layer of negatively charged Cu in reduction reactions. Na will stably locate near the solid-liquid interface with the increase of reduction voltage.

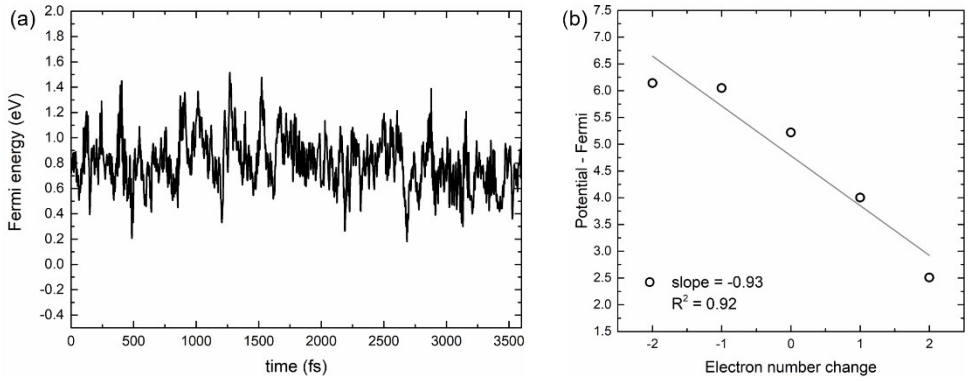

Figure S4. (a) The Fermi level of the neutral Cu electrode in 3600 fs MD simulation in an explicit water model simulation with 3x3 Cu (111) supercell. (b) Linear relationship of the difference of middle solvent layer potential and Fermi energy versus electron number change in an implicit solvent model simulation with 3x3 Cu (111) supercell.

Since the fixed potential calculation is rather expensive (and need to use the three layers model with Poisson-Boltzmann equation), the fixed charge calculation is a more feasible option (consider the large number of steps necessary in the MD simulation). Therefore, the fixed charge calculation, instead of a fixed potential grand canonical calculation was used in this work. That means that the electrode potential is not constant because of fluctuations in the chemical environment, which causes a challenge to calibrate the relationship between charge and potential. However, as we shown in our recent work, the most important effects of the fixed potential method can be captured by using a relevant fixed charge.[14] The important thing is to calibrate the relationship between charge and potential. We should note that the electrode potential represented by the Fermi energy of the electrode does not change significantly

in MD simulation. In Fig. S4a, the Fermi energy has an RMS variation of 198 meV during a typical MD simulation, and after the average over the simulation time, the uncertainty is only about 16 meV (with decay time tau = 23 fs estimated from the fluctuation correlation function and that time is used to estimate the error after average, by multiplying the RMS variation value by sqrt(tau /t_tot), t_tot=3600 fs. This procedure is described in the above *Notes for error bar of the average force* part. Such fluctuation, just like the fluctuation we have when estimating the simulation temperature in a NVT simulation, can be considered as part of the features in a MD simulation, thus should be acceptable. Overall, this means we can use a fixed charge simulation to represent the fixed potential simulation given that the charge-potential relationship can be calibrated.[14] To better calibrate this relationship between the extra charge and the potential change without the influence of the fluctuations, we have now used the implicit water model. For this, we have calculated the difference between the water layer middle potential and Fermi energy with implicit solvent model (VASPsol).

In the Fig. S4b, electron number change of Cu exhibits a strong linear relationship with the difference of middle vacuum layer potential and Fermi energy, with $R^2 = 0.92$. The slope is -0.93, thus we have:

$$U = U_{PZC} - 0.93 * \Delta n$$

where the U_{PZC} is the potential of zero charge (-0.3 V) of Cu (111),[15-16] and Δn is the change of electron number in Cu. According to this equation, we can obtain Cu slab with 1.56 V, 1.37 V, 1.10 V, 0.91 V, 0.63 V, -1.23 V, -2.16 V electrode potential vs SHE by changing -2, -1.8, -1.5, -1.3, -1, 1, 2 electrons in Cu, respectively.

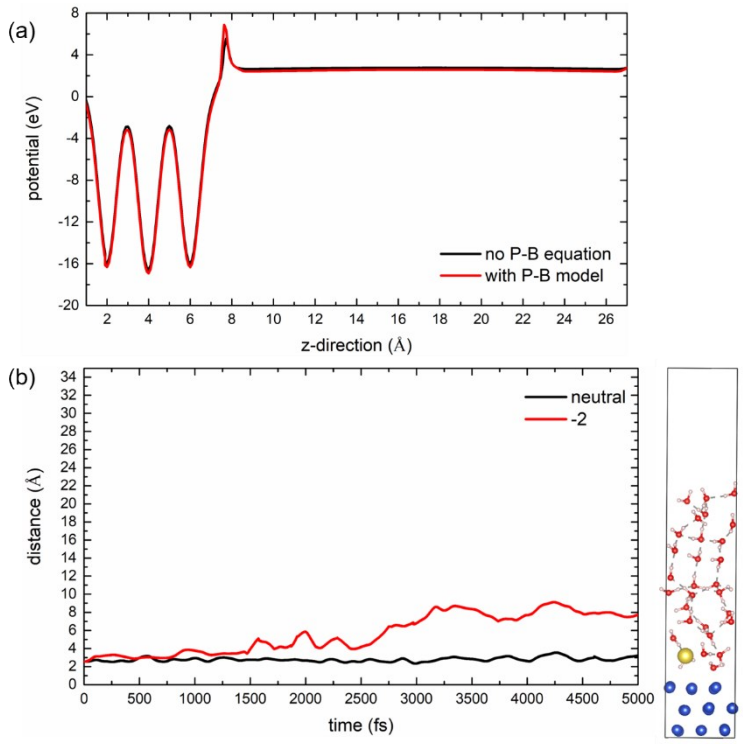

Figure S5. (a) The potential for Cu (111) with 2 electrons deprived using the implicit solvent model without Poisson-Boltzmann equation (black line) and with Poisson-Boltzmann model with 0.1 mole salt (red line, Debye wave length of 9.5 Å). (b) Na^+-first layer Cu distance versus time on neutral structure and the structure with 2 electrons deprived, with the last structure image of MD simulation of neutral structure on the right.

The charged systems in this work were handled using the uniform background countercharge in VASP. Here, we want to discuss the possible impacts by this uniform background countercharge. In practice, the effect by the uniform background countercharge can be rather small due to the large dielectric constant of water (epsilon=78). Note, our explicit water calculation has the same treatment as the implicit solvent model (without the Poisson-Boltzmann equation) in regard to the back ground charge (both use the back ground charge). The difference only exists when the Poisson-Boltzmann equation is used in the solvent model. To illustrate the background charge effect, Fig. S5a shows the potential in the water region with 2 electrons deprived (the maximum charge used in our calculation) in the electrode using the implicit solvent model, but not the Poisson-Boltzmann equation. As we can see, in practice, beyond the thin Helmholtz layer, the potential is relatively linear/flat. That means the effect of the uniform charge is small (a large uniform charge without screening can make the potential curve bended). Fig.S5a also shows the potential profile using the implicit solvent model with Poisson-Boltzmann equation. Although they represent two different treatments for the compensation charge (one uniform, one following implicit the Boltzmann distribution for the counter-ion), the potential profiles

are quite similar (due to the large screening effect of the water). Thus, the charge background is not a major issue.

To further illustrate this, we have carried out additional explicit AIMD calculations. Since our goal is to study the explicit water effect, we obviously cannot use the implicit water model throughout the water region. So, one choice is to have a Cu/explicit-water/solvent-model structure. In this hybrid model, due to the use of Poisson-Boltzmann solvent model, there is no need to have a uniform charge background. We like to point out that, this model is actually not more natural than the uniform background model in our original calculation. It artificially prevents the salt counter ion from entering the explicit water region, thus it is artificial by its own way. Nevertheless, we use it here to show, how large is the difference under the different back ground charge (or said counter charge) treatments.

To do that, we have added 10 Å vacuum layer with VASPsol (with Poisson-Boltzmann equation, Debye wave length of 3 Å) to counteract the extra charge on the electrode based on our original 20 Å vacuum space with explicit water. 5 ps AIMD was carried out for the neutral structure and the structure with 2 electrons deprived. As shown in Fig. S5b, for the neutral structure, Na^+ is still stably stay at 3 Å above the first layer of Cu, exactly the same as in our original simulation. While with the 2 electrons deprived case, the Na^+ escapes away from the metal surface and stay at about 8 Å away from the metal surface. This is slightly smaller than the 10 Å in our original calculation. But roughly, they are both at the center of their respective water regions. The fact they are all escape from the 3 Å position to the bulk water is the same. The important thing is that, when the Na^+ is close to the Cu surface, the results are the same, and they are not affected by the different back ground charge treatment. Thus, in the rest of the simulation, we will just use the Cu/explicit-water structure model.

5. The Tables in the supporting information (Table S1 ~ Table S2)

Table S1. The time-averaged 1s-core level of Oxygen for each water layer for clean Cu with explicit water and no cation. The fermi energy was set to be 0.

Water layer	1	2	3	4
Core level (eV)	-506.394	-505.924	-505.693	-505.633

Table S2. Mean force of Na towards z axis, free energy and Boltzmann distribution of Na with the falling from infinity to the interface in thermodynamics integration.

Na-Cu distance	Mean force/ (±)error	Free energy	Distribution
11.35	-0.028/0.019	0	1
10.19	-0.013/0.026	-0.024	2.54
9.51	-0.0086/0.019	-0.032	3.38
9.10	-0.018/0.021	-0.037	4.15
8.96	-0.018/0.017	-0.039	4.55
8.82	-0.092/0.021	-0.047	6.09
8.48	-0.055/0.021	-0.072	16.09
8.14	0.058/0.026	-0.071	15.81
7.80	0.14/0.015	-0.039	4.44
7.63	0.075/0.019	-0.021	2.22
7.46	-0.042/0.023	-0.018	1.99
7.22	0.036/0.026	-0.019	2.05
6.98	0.031/0.023	-0.010	1.50
6.50	0.058/0.029	0.011	0.65
6.02	0.054/0.024	0.038	0.23
5.54	0.031/0.021	0.059	0.10
5.48	-0.094/0.017	0.057	0.11
5.42	-0.14/0.019	0.049	0.15
4.73	-0.11/0.020	-0.035	3.87
4.05	-0.095/0.021	-0.11	58.16
3.37	-0.091/0.015	-0.17	677.40
2.96	-0.069/0.016	-0.20	2400.75
2.76	0.091/0.012	-0.20	2204.05
2.55	0.10/0.013	-0.18	1019.16

Reference

(1) G. Kresse and J. Furthmüller, *Comput. Mater. Sci.,* 1996, **6**, 15-50.

(2) G. Kresse and J. Furthmüller, *Phys. Rev. B,* 1996, **54**, 11169.

(3) P. E. Blöchl, *Phys. Rev. B,* 1994, **50**, 17953.

(4) J. P. Perdew, K. Burke and M. Ernzerhof, *Phys. Rev. Lett.,* 1996, **77**, 3865.

(5) J. P. Perdew, M. Ernzerhof and K. Burke, *J. Chem. Phys.,* 1996, **105**, 9982-9985.

(6) S. Grimme, J. Antony, S. Ehrlich and H. Krieg, *J. Chem. Phys.,* 2010, **132**, 154104.

(7) D. Frenkel and B. Smit, Understanding molecular simulation: from algorithms to applications; Elsevier, 2001; Vol. 1.

(8) J. G. Kirkwood, *J. Chem. Phys.,* 1935, **3**, 300-313.

(9) A. Grossfield, and D. M. Zuckerman, *Annu. Rep. Comput. Chem.,* 2009, **5**, 23-48.

(10) X. Liu, P. Schlexer, J. Xiao, Y. Ji, L. Wang, R. B. Sandberg, M. Tang, K. S. Brown, H. Peng, S. Ringe and C. Hahn, *Nat. Commun.*, 2019, **10**, 32.

(11) X. Liu, J. Xiao, H. Peng, X. Hong, K. Chan and J. K. Nørskov, *Nat. Commun.*, 2017, **8**, 15438.

(12) T. Ludwig, J. A. Gauthier, K. S. Brown, S. Ringe, J. K. Nørskov, K. Chan, *J. Phys. Chem. C.*, 2019, **123**, 5999-6009.

(13) K. Jiang, R. B. Sandberg, A. J. Akey, X. Liu, D. C. Bell, J. K. Nørskov, K. Chan and H. Wang, *Nat. Catal.*, 2018, **1**, 111-119.

(14) G. Gao, and L.W. Wang, *J.Catal.*, 2020, **391**, 530.

(15) J. J. McMullen and N. Hackerman, *J. Electrochem. Soc.,* 1959, **106**, 341.

(16) G. J. Clark, T. N. Andersen, R. S. Valentine and H. Eyring, J. *Electrochem. Soc.*, 1974, **121**, 618.